

# Scaling laws for slippage on superhydrophobic fractal surfaces

C.Cottin-Bizonne,<sup>\*</sup> C. Barentin,<sup>†</sup> and L. Bocquet<sup>‡</sup>  
*LPMCN; Université de Lyon; Université Lyon 1 and CNRS,  
UMR 5586; F-69622 Villeurbanne, France*

(Dated: April 6, 2022)

We study the slippage on hierarchical fractal superhydrophobic surfaces, and find an unexpected rich behavior for hydrodynamic friction on these surfaces. We develop a scaling law approach for the effective slip length, which is validated by numerical resolution of the hydrodynamic equations. Our results demonstrate that slippage does strongly depend on the fractal dimension, and is found to be always smaller on fractal surfaces as compared to surfaces with regular patterns. This shows that in contrast to naive expectations, the value of effective contact angle is not sufficient to infer the amount of slippage on a fractal surface: depending on the underlying geometry of the roughness, strongly superhydrophobic surfaces may in some cases be fully inefficient in terms of drag reduction. Finally, our scaling analysis can be directly extended to the study of heat transfer at fractal surfaces, in order to estimate the Kapitza surface resistance on patterned surfaces, as well as to the question of trapping of diffusing particles by patchy hierarchical surfaces, in the context of chemoreception.

PACS numbers: 68.08.-p, 68.15.+e, 47.61.-k, 47.63.Gd

## I. INTRODUCTION

Superhydrophobic (SH) surfaces have raised a considerable interest over the recent years [1, 2]. A SH surface is typically characterized by a contact angle exceeding  $150^\circ$ , which results from the combination of bare hydrophobicity and micro- and nano- scale roughness on the surfaces. This exceptional wetting property has motivated numerous studies to rationalize superhydrophobicity and device versatile SH materials, as well as to explore its implication in the context of transport and fluid dynamics [2–12]. In particular, patterned SH surface were shown to exhibit low friction – superlubricating – properties in the Cassie state [13], *i.e.* when the liquid interface lies at the top of the roughness and thus strongly reduces the direct solid-liquid contact area [14–16]. This drag reduction phenomena is associated with a large slippage of the fluid at the SH surface [7–9]. The quantity of interest is accordingly the effective slip length  $b_{\text{eff}}$ , entering the Navier boundary condition [17, 18] for the averaged velocity field at the surface :  $b_{\text{eff}}\partial_z v = v_w$ , where  $v_w$  is the slip velocity at the wall, averaged over the lateral surface [16].

In this paper, we study the friction properties on multiscale fractal SH surfaces. Fractal SH surfaces were indeed shown to exalt superhydrophobicity [19, 20]. Furthermore the fractal nature of the interface was shown to enhance the robustness of the Cassie state with respect to the Wenzel state (with the liquid impregnating the roughness), as compared to simple regular structures such as periodic stripes or pillars [21–24]. However how

the fractal, multiscale nature of the interface impacts transport and hydrodynamic slippage remains largely unknown. Recently Feuillebois *et al.* could obtain rigorous bound on the slip length on Hashin-Shtrikman fractals in a thin channel geometry [25]. Another contribution showed that for a SH interface made of pillars, randomness in the post structure does weaken the drag reduction as compared to periodic structure [26]. Also, recent experiments by Lee and Kim showed that a hierarchical surface with nanoposts lying on the top of microposts does not necessarily lead to an increase in slip length [27]. This points to the subtle connection between surface slippage and the structure of the underlying surface.

A key difficulty is that there is not general analytical theory describing hydrodynamic flows on composite surfaces. Therefore, analytical results for the slip length could only be obtained in specific and simple geometries with regular stripes [14–16], while asymptotic calculations on regular 2D post structures allowed to rationalize the limiting behavior of the slip length in the low surface fraction regime [28]. In this context, solving the Stokes equation with a fractal structure of boundary conditions appears hopeless. To bypass this difficulty, we resort to a scaling law approach for the fluid dynamics, which we put forward in a previous paper for regular surfaces [29]. In particular, this allows us to derive simple scaling laws to characterize the slippage properties on hierarchical – fractal – surfaces as a function of the roughness characteristics: surface solid fraction  $\phi_s$  and fractal dimension  $d_f$  of the interface. The validity of this approach is then validated on the basis of numerical resolution of the Stokes equations.

The main results of the present study are that: for 2D structures

- The fractal dimension  $d_f=1$  corresponds to a change of behavior of the friction: for fractal dimension lower than 1,  $d_f < 1$ , the effective slip length

<sup>\*</sup> cecile.cottin-bizonne@univ-lyon1.fr;  
<http://www-lpmcn.univ-lyon1.fr/interfaces/fluides/>

<sup>†</sup> catherine.barentin@univ-lyon1.fr

<sup>‡</sup> lyderic.bocquet@univ-lyon1.fr; <http://www-lpmcn.univ-lyon1.fr/~lbocquet>

diverges in the low solid fraction limit  $\phi_s \rightarrow 0$ , while for  $d_f > 1$ , the effective slip length saturates to a finite value at low solid fraction. For  $d_f = 1$  the divergence is logarithmic as  $\phi_s \rightarrow 0$ .

- For  $d_f < 1$  the scaling approach predicts that the effective slip length behaves as  $b_{\text{eff}} \sim \phi_s^{-\alpha}$  with an exponent  $\alpha = (1 - d_f)/(2 - d_f)$  which depends directly on the fractal dimension  $d_f$  of the interface. The explicit prefactor for this scaling behavior can be calculated analytically, leading to the prediction  $b_{\text{eff}} \simeq \frac{3}{8}L \left(\frac{4}{\pi}\phi_s\right)^{-\alpha}$  for circular posts and valid in the low  $\phi_s$  regime. This generalizes for fractal surfaces the asymptotic result obtained by Davis and Lauga for circular posts on a square array (with  $\alpha = 1/2$ ) [28].
- For a given solid fraction  $\phi_s$ , regular surfaces (periodic stripes or pillars) lead to higher slip lengths than for fractal surfaces. The difference between the two types of surfaces is enhanced at small solid fraction.
- The value of the effective contact angle  $\theta_{\text{eff}}$  (characterizing the wetting properties) is not sufficient to quantify the amount of slippage on the surface: the effective contact angle is not a relevant parameter to infer the slipperiness of a given surface.

For 1D structures, the slip length for hierarchical fractal surfaces does saturate to a finite value at small surface fraction  $\phi_s$  and is therefore always far below the result for regular stripes.

Here we consider hierarchical fractal SH surfaces obtained by the periodic repetition of a unit cell. We denote by  $L$  the period of the structure. We make an iterative geometric construction of the unit cell. For the first iteration ( $n=1$ ) the unit cell is divided in  $p$  parts in each direction among which  $k$  patches represent a solid surface, the other parts corresponding to the gas interface with negligible friction. At all further iterations  $n > 1$ , each solid patch is replaced by the pattern defined at the first iteration, with the initial period  $L$  replaced by the smaller scale of the solid patch. On Fig.1 we have represented two examples of the unit cells of hierarchical SH surfaces that we have studied in 2D (a) and in 1D (b) at the first iteration  $n=1$  (a1 and b1) and at the second iteration  $n=2$  (a2 and b2). Using this recursive construction for the hierarchical multi-scale structure, there is self similarity only over a finite range of scales, the “true” fully fractal surface being obtained in the limit  $n \rightarrow \infty$ . The fractal dimension for such structures is:

$$d_f = \frac{\log k}{\log p}. \quad (1)$$

The initial solid fraction (for  $n=1$ )  $\phi_0$ , is equal in 1D to  $\phi_0 = \frac{k}{p}$ , and in 2D to  $\phi_0 = \frac{k}{p^2}$  (here patches with a squared geometry are considered). The solid fraction at the second iteration  $n=2$  is then:  $\phi_{s2} = (\phi_0)^2$  and more

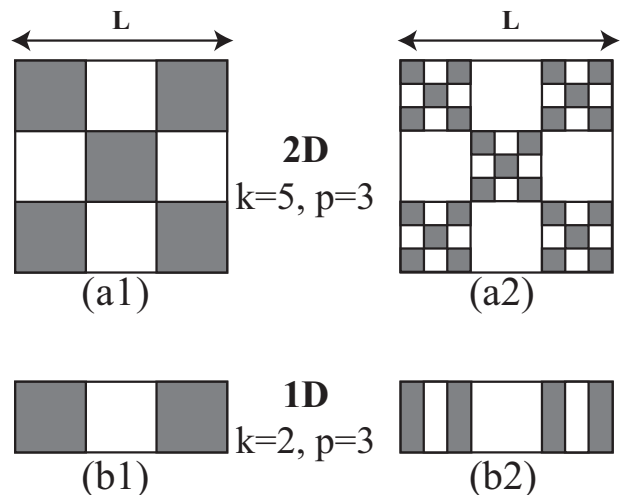


FIG. 1. Iterative construction of the hierarchical surfaces considered in this study, in 2D (a1, a2) and 1D (b1, b2). Filled patches correspond to the solid-liquid interface, while open patches correspond to the gas-liquid interface. The local boundary conditions are no-slip on the filled patches and perfect slip on the open patches. In 2D for  $k=5$ ,  $p=3$ , (a1) first iteration  $n=1$  and (a2) second iteration  $n=2$ . In 1D for  $k=2$ ,  $p=3$ : (b1)  $n=1$  and (b2)  $n=2$ .

generally the solid fraction at an iteration  $n$  is:  $\phi_s = (\phi_0)^n$ .

## II. A SCALING LAW APPROACH

We first present the basis of the scaling law approach which we developed to evaluate the slip length on SH fractal surfaces. The starting point is a hierarchical relationship which we proposed in Ref. [29], and showing that for a SH surface of roughness periodicity  $L$ , a (small) solid fraction  $\phi_s$  and slip length  $b_s$  on the solid at the top of the roughness, the effective slip length  $b_{\text{eff}}$  takes the following expression:

$$b_{\text{eff}} \underset{\phi_s \rightarrow 0}{\simeq} b_0 + \frac{b_s}{\phi_s}. \quad (2)$$

In this equation,  $b_0$  stands for the slip length for the same geometry when there is no slip on the solid at the top of the roughness ( $b_s = 0$ ) [30]. Typically we showed that  $b_0 \sim a/\phi_s$  where  $a$  the typical lateral size of the roughness feature.

We briefly recall the physical idea underlying this relationship. It is obtained by identifying the averaged friction force on the surface, which is by definition  $F_s = \mathcal{A}\eta U/b_{\text{eff}}$  – with  $\mathcal{A}$  the lateral area and  $U$  the slip velocity –, with the total viscous force acting on the top of the solid roughness (say, posts or stripes), which writes  $F_\eta = \eta\phi_s \langle \dot{\gamma} \rangle$ , with  $\langle \dot{\gamma} \rangle$  the average shear-rate on a single roughness feature. As proposed in Ref. [29], a simple estimate for this quantity is  $\langle \dot{\gamma} \rangle \sim U/(a + b_s)$ , with

$a$  the typical size of the solid roughness feature. This force balance leads to  $b_{\text{eff}} \sim a/\phi_s + b_s/\phi_s$ , and thus to Eq.(2). Note that this derivation neglects hydrodynamic interactions between different roughness features and is expected to be valid in the limit of small solid fraction  $\phi_s$ . In Ref. [29], we have checked in detail the validity of the above analysis and of Eq.(2).

Here we extend this scaling analysis to the case of hierarchical fractal SH surfaces: the main idea is to use Eq.(2) as a hierarchical relation between the different scales of the roughness, with  $b_s$  characterizing the slippage of the patch at lower scales.

### A. Wettability and contact angle

Let us first consider the wettability of these surfaces. This is usually characterized by the effective contact angle  $\theta_{\text{eff}}$  of a droplet on the surface. Using Cassie-law,  $\theta_{\text{eff}}$  is obtained in terms of ratio between the solid-liquid and gas-liquid contact area. Introducing  $\phi_s$  the solid surface fraction, one has

$$\cos\theta_{\text{eff}} = \phi_s(1 + \cos\theta_0) - 1 \quad (3)$$

with  $\theta_0$  the contact angle on the bare, smooth surface with the same chemical characteristics. As pointed above, the solid fraction is given by  $\phi_s = \phi_{s1} = \phi_0$  at step  $n = 1$ , while at step  $n = 2$ ,  $\phi_s = \phi_{s2} = \phi_0^2$ . For a surface characterized by a hierarchy of  $n$  successive scales, then  $\phi_s = \phi_{sn} = \phi_0^n$ . Going up in the hierarchy, the solid fraction  $\phi_s$  thus decreases and the contact angle on those hierarchical fractal surfaces converges *exponentially* towards  $180^\circ$ :

$$\cos\theta_{\text{eff}} + 1 \xrightarrow[n \rightarrow \infty]{} 0 \quad (4)$$

Let us now turn to the slippage properties.

### B. Slippage on a two scale roughness

To illustrate the approach, we begin by studying the simplest hierarchical surface obtained with two steps in the iteration process ( $n=2$ ), i.e., two roughness scales as represented in Fig.1 (a2) and (b2). Such hierarchical surfaces are now accessible from experiments thanks to the progress in nanofabrication techniques [21, 23].

Let us introduce  $b_1$ , the effective slip length obtained after one iteration  $n=1$ , see Fig.1 (a1) and (b1). A key remark is that, when going from the first  $n = 1$  to the second step  $n=2$ , the higher-level structure inside each main solid patch is equivalent to the initial bare structure at  $n = 1$ , up to a rescaling of the size by  $1/p$  ( $p$  being the size ratio between two scales, as defined above).

Using Eq.2, we then deduce that the effective slip length is equal to:

$$b_2 = b_1 + \frac{b_1}{p\phi_0}, \quad (5)$$

where we recall that  $\phi_0$  is the solid fraction at the initial scale, in Fig.1(a1)-(b1). For 1D structures like in Fig.1(b1),  $\phi_0 = k/p$ , so that one obtains

$$b_2 = b_1 \times \left(1 + \frac{1}{k}\right), \quad (6)$$

For 2D structures like in Fig.1(a1),  $\phi_0 = k/p^2$  and

$$b_2 = b_1 \times \left(1 + \frac{p}{k}\right), \quad (7)$$

The slip length is obviously higher at the second iteration. There is an increase in slip length for hierarchical “fractal” SH surfaces and this increase is larger for 2D structures than 1D. Such a difference between the 1D and 2D structures was already pointed out for regular periodic SH surfaces [29].

### C. Slippage on hierarchical fractal surfaces

Now, “real” SH fractal surfaces are composed by an infinite number of iterations, or at least by a large number  $n$  of it, so that the fractal dimension is defined over a broad range of scales. To estimate the slip length, we extend the previous analysis for any number of iterations.

At a subsequent iteration  $n + 1$ , the solid patches are divided once again into  $p$  parts, see Fig.1. As an alternative view, one may consider that the system at the subsequent iteration  $n + 1$  is made by first assembling  $k$  systems obtained at the previous iteration  $n$  in order to gather a structure with the correct geometry, and then perform a global rescaling by  $1/p$  to obtain the desired structure at step  $n + 1$ . Accordingly, the structure inside the largest patches at the iteration  $n + 1$  can be seen as the previous structure at iteration  $n$ , up to a rescaling factor  $p$  between scales.

One may deduce directly the recursion relationship for the slip length from the above procedure. At scale  $n + 1$  the slip length over each of the largest patches is then  $b_n/p$  (since we have gathered structures from iteration  $n$  and rescaled by  $1/p$ ; remind that the slip length does scale with the global lateral size of the system). Now using Eq. 2, the slip length  $b_{n+1}$  at iteration  $n + 1$  can be deduced as a function of  $b_n$  as:

$$b_{n+1} = b_1 + \frac{1}{\phi_0} \times \frac{b_n}{p} \quad (8)$$

The last term thus gathers all the slippage effects on all above scales  $\geq n$  in the hierarchy;  $b_1$  is the slip length of the elementary structure, as in Fig.1(a1)-(b1). This can be rewritten as

$$b_{n+1} = b_1 + b_n x \quad \text{with} \quad x = \frac{1}{p\phi_0}. \quad (9)$$

so that

$$b_n = b_1 \times \sum_{k=0}^{n-1} x^k = b_1 \frac{1 - x^n}{1 - x} \quad (10)$$

Depending on the parameter  $x$ , different scenarios occur:

- For  $x < 1$ , the sum in Eq.(10) converges exponentially to a finite value in the limit  $n \rightarrow \infty$ :

$$b_\infty = b_1 \times \frac{1}{1-x} \quad (11)$$

- For  $x = 1$ , the effective slip length at an iteration  $n$  is proportional to  $n$ ,  $b_n = n \times b_1$ . Now, replacing the scale index  $n$  by the corresponding solid surface  $\phi_s$  at the corresponding scale,  $\phi_s = \phi_0^n$  so that  $n = \log \phi_s / \log \phi_0$ , then one gets

$$b_{\text{eff}}(\phi_s) = b_n = b_1 \times \frac{\log \phi_s}{\log \phi_0}. \quad (12)$$

The slip length thus diverges *logarithmically* with the solid fraction  $\phi_s$  in the limit of small  $\phi_s$ .

- For  $x > 1$ , the largest term in Eq.(10) dominates the effective slip length, so that the slip length has the asymptotic expression in the limit  $n \rightarrow \infty$  ( $\phi_s \rightarrow 0$ )

$$b_{\text{eff}}(\phi_s) = b_n \simeq \frac{b_1}{x-1} \times x^n, \quad (13)$$

with  $n = \frac{\log \phi_s}{\log \phi_0}$ .

As a side note, one may remark that these results could be generalized to the situation with a finite slip length  $b_0$  on the liquid-gas interface. Our present results thus propose an upper bound for the effective slip length in the latter situation. We leave this generalization for future work.

#### D. Discussion: 1D/2D hierarchical surfaces versus regular surfaces

We now summarize the different scaling expression for the slip length for 1D and 2D structures and for the different values of  $x$ . A key quantity is the fractal dimension of the structure,  $d_f = \frac{\log k}{\log p}$ .

- For 1D structure,  $x = 1/k$  and  $k < p$ , so that  $x \leq 1$  and  $d_f < 1$ .
- For 2D structure,  $x = p/k$  and  $k < p^2$  so that one finds three different cases: for  $x < 1$ ,  $1 < d_f < 2$ ; for  $x = 1$ ,  $d_f = 1$ ; and for  $x > 1$ ,  $d_f < 1$ .

##### 1. 1D structures

In 1D, two situations occur:

- For  $0 < d_f < 1$  ( $x < 1$ ), then  $b_\infty = b_1 \frac{k}{k-1}$ , and the maximum value of  $b_\infty/b_1$  is 2 (for  $k = 2$ ). This shows that the hierarchical fractal geometry only generates a

maximal amplification by a factor of two for the slip length as compared to a regular SH surface defined with only one roughness scale. In this regime, the slip length does not diverge in the limit of perfect superhydrophobicity,  $\theta_{\text{eff}} = 180^\circ$ , or  $\phi_s = 0$ .

- The peculiar case  $d_f=0$  ( $x = 1$ , *i.e.*  $k=1$ ) corresponds to a flow parallel to stripes. We recover in this case the slow logarithmic divergence of the slip length with the solid fraction  $b_n \sim \log \phi_s^{-1}$  as obtained in Refs. [14]. This result is non trivial as in the present approach we do not explicitly take into account the hydrodynamics interactions between stripes.

##### 2. 2D structures

In 2D, a variety of situations occurs depending on the ration  $x = p/k$ . The latter parameter quantifies the dense or sparse character of the solid filling on the surface.

- For  $1 < d_f < 2$  ( $x = p/k < 1$ ), the solid filling is quite dense – this is the situation depicted in Fig.1(a1)-(a2) –. In this regime, the slip length of the SH hierarchical surface saturates to a value  $b_\infty = b_1 \frac{k}{k-p}$  in the limit of low  $\phi_s$ .
- For  $d_f = 1$  ( $x = p/k = 1$ ), we find a logarithmic divergence of the slip length with the solid fraction  $b_n = n \times b_1 = \frac{\log \phi_s}{\log \phi_0} b_1$ . We find the same divergence as for a 1D regular SH surface of stripes.
- For  $d_f < 1$  ( $x = p/k > 1$ ), the solid filling is sparse. In this case the effective slip length diverges as a power law of the solid fraction. Using Eq.13, we get for large  $n$ , *i.e.* small  $\phi_s$ :

$$b_{\text{eff}}(\phi_s) = b_n \approx \frac{1}{x-1} b_1 \times \phi_s^{-\frac{1-d_f}{2-d_f}} \quad (14)$$

with again  $d_f = \frac{\log k}{\log p}$  the fractal dimension.

We can compare the scaling behavior predicted in this last regime with the one obtained for a SH surface made out of a bidimensional regular pattern of posts for which the slip length behaves for small  $\phi_s$  as  $b_{\text{eff}} \sim \frac{L}{\sqrt{\phi_s}}$  [29]. Since  $\frac{1-d_f}{2-d_f} < \frac{1}{2}$ , this shows that for a given solid fraction  $\phi_s$ , the slip length on the periodic patterns of post is larger than of 2D SH fractal surfaces. This is a counter-intuitive result, which shows that fractality, though strongly increasing the non-wettability, is far less efficient in enhancing dynamic properties.

##### E. Alternative scaling law approach in the dilute regime

Here we propose a simpler, alternative description to account for the scaling laws above. We focus on the case

of a sparse solid filling in 2D, corresponding to  $d_f < 1$  and  $x$  larger than unity.

Then in the dilute regime, when the hydrodynamics interactions can be neglected, the effective slip length  $b_{\text{eff}}$  can be estimated directly from the calculation of the viscous friction force  $F$  of a liquid of viscosity  $\eta$  on a unit cell of size  $L$  of the hierarchical SH surface at a given step  $n$ . We consider a flow leading to a slip velocity  $U$  at the surface. By definition of the slip length, the friction force on the surface takes the expression:

$$F = \eta \frac{U}{b_{\text{eff}}} L^2 \quad (15)$$

with  $\eta$  the shear viscosity of the fluid. Now the friction force can be calculated as the sum of the forces on each solid post. Separating the scale of the post from the lateral scale between the post, this friction force can be calculated from the Stokes equation applied to the posts considered as individual stationary solid object in a fluid moving at velocity  $U$  far from it:

$$F_\nu = \sum_{\text{solid patches}} \chi \eta a_n U \quad (16)$$

Here the sum runs over all the solid patches on the surface, with characteristic lateral size  $a_n$  at the smaller scale  $n$ ; here  $\chi$  is the numerical prefactor for the Stokes law. The latter depends only on the geometrical characteristics of the solid post. For example for a solid disk with radius  $a$ , one has  $\chi = \frac{1}{2} \times \frac{32}{3}$  [31]. The factor  $\frac{32}{3}$  comes from the Stokes flow calculation around a disk, as calculated in Ref.[31], while the 1/2 prefactor stems from the fact that only the upper-half of the disk undergoes friction.

Now at an iteration  $n$ , the lateral size of the solid post scales like  $a_n \sim L/p^n$  and there are  $k^n$  of such posts. Altogether equating the two expressions for the friction force, we thus obtain the scaling law for the slip length in the dilute regime:

$$b_{\text{eff}} \sim L \left( \frac{p}{k} \right)^n \quad (17)$$

Using the definition of  $\phi_s$  and  $d_f$  this leads to the scaling behavior

$$b_{\text{eff}} \sim \phi_s^{-\frac{1-d_f}{2-d_f}} \quad (18)$$

and we recover the same result as in Eq.14, obtained with the previous hierarchical approach.

Now we finally remark that further insight can be obtained from the above analysis to predict the prefactor of the previous scaling behavior. We will focus on posts with disk shape for which the prefactor  $\chi$  in the viscous force, in Eq.(16), can be exactly calculated, as pointed out above.

We first start by noting that applying a similar analysis to a *regular* square pattern of disk-like posts yields  $b_{\text{eff}} = 3/16 \times L^2/a$  with  $a$  the disk radius, and we used  $\chi = 16/3$

for the disks as discussed above. Using  $\phi_s = \pi a^2/L^2$  for the surface fraction, one gets the following expression for the slip length

$$b_{\text{eff}} \simeq \frac{3\sqrt{\pi}}{16} \frac{L}{\sqrt{\phi_s}} \quad (19)$$

The prefactor  $\frac{3\sqrt{\pi}}{16}$  is the *exact one* calculated by David and Lauga [28] using asymptotic expansions and confirmed in numerical resolution of the hydrodynamic problem [29]. This demonstrates the power of the scaling approach in deriving relevant expression for slip lengths. The above analysis can also immediately extended to predict the slip length on an array of posts of any shape (*e.g.* ellipsoids) and any pattern symmetry.

Coming back to the hierarchical pattern, a similar analysis for disk-like posts allows to show that  $b_{\text{eff}}/L = 2/\chi \times x^n$  with  $\chi = 16/3$  for disks. Using  $\phi_s = \frac{\pi}{4}(k/p^2)^n$ , where the  $\pi/4$  factor takes into account the disk shape of the posts, this equation can be rewritten as

$$b_{\text{eff}} \simeq \frac{3}{8} L \left( \frac{4}{\pi} \phi_s \right)^{-\frac{1-d_f}{2-d_f}} \quad (20)$$

The previous result for a regular square pattern of disk posts is exactly recovered by putting  $d_f = 0$  in this equation.

Furthermore this result can be rewritten as  $b_{\text{eff}} = b_1 \times x^{n-1}$ , with  $b_1 = \frac{2L}{\chi}x$ : this expression is identical to Eq. (13) obtained by the alternative iterative derivation, for  $x \gg 1$  (sparse structure). This demonstrates the equivalence between the direct and hierarchical calculations for the slip length on fractal surfaces.

### III. NUMERICAL RESULTS

In order to assess the validity of the above scaling approach, we perform a numerical resolution of the full hydrodynamic equations complemented by the composite boundary conditions on the hierarchical surface, as sketched for example in Fig.1. Specifically, the hydrodynamic velocity field obeys Stokes equation in the bulk, with a no-slip boundary condition on the solid patches and a perfect slip boundary condition on the remaining liquid-gas interface (open patches in Fig.1).

To this end, we follow the numerical approach developed by Cottin-Bizonne *et al.* in Ref. [32]. We only recall here the basic steps of this approach, and a more detailed description can be found in [32]. A shear flow is considered over a composite surface characterized by a heterogeneous slip length pattern. The boundary is modeled by a pattern of local slip lengths on a planar surface. The hydrodynamic equations for flow profile are rewritten analytically in terms of a boundary integral method, which is then solved numerically. The effective slip length is deduced from the asymptotic flow profile far from the surface.

Using this numerical approach, we calculate the effective slip length  $b_{\text{eff}}$  for SH hierarchical fractal surfaces as the ones represented on Fig.1. The computed slip lengths  $b_{\text{eff}}/L$  will be calculated for different SH hierarchical surfaces, for both 1D and 2D structures, as well as for different values of  $k$  and  $p$  and iteration steps,  $n$ . The numerical values will then be compared with the predictions obtained using the scaling law approach.

In practice, due to the large range of spatial length scales involved, the numerical calculations require a higher discretization than the one performed with a regular square lattice of solid patches as considered in [29]. The calculations involve substantially larger matrices, which limits the range of fractal surfaces that can be considered. Consequently, the numerical method is limited to only a few iterations as shown in Fig.3 and 5. This will however prove sufficient to explore the main tendencies predicted by the hierarchical approach.

### A. Numerical results for slippage over hierarchical 2D structures

We have first plotted in Fig.2 the numerical results for the effective slip length  $b_{\text{eff}}/L$  as a function of the solid fraction  $\phi_s$ , for SH surfaces made out of both periodic posts on a square lattice and hierarchical fractal surfaces obtained with different parameters  $k$  and  $p$ . A first striking result emerging from this plot is that the surfaces with regular structures of posts are far better than all the fractal surfaces in terms of slip length for a given solid fraction.

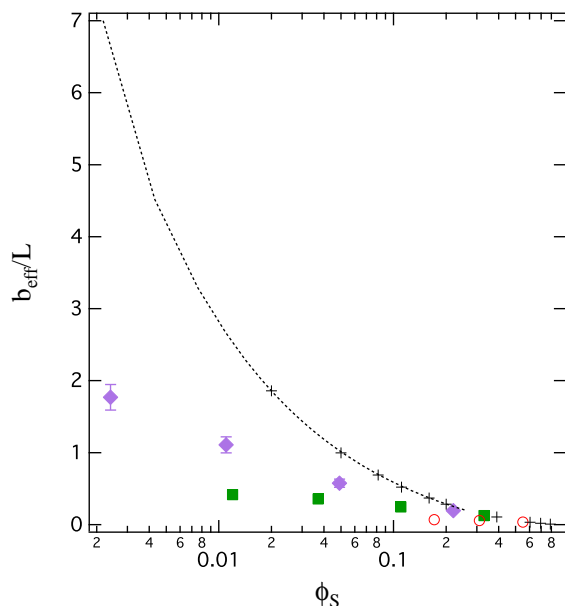
The detailed comparison between the numerical results and the incremental scaling laws is then shown in Fig.3. A general conclusion from this plot is that the scaling predictions in the previous section are in good agreement with numerical results.

(i) Case  $x = p/k < 1$  i.e. fractal dimension  $d_f > 1$ : two cases have been solved numerically with hierarchical structures corresponding to  $\{k,p\}=\{5,3\}$  and  $\{k,p\}=\{6,3\}$ . At the first iteration  $n = 1$ , these structures have a surface fraction of  $\phi_0 = 0.55$  and  $\phi_0 = 0.66$  respectively. For further iterations, the solid fraction obeys  $\phi_s(n) = \phi_0^n$ .

The scaling predictions in this case suggest a finite slip length, which saturates at small  $\phi_s$ . This is indeed the tendency shown by the numerical results.

To be more quantitative, we use the results for the slip length in Eq.10:  $b_n = b_1(1 - x^n)/(1 - x)$  with  $n = \log(1/\phi_s)/\log(p^2/k)$ . One has to fix the numerical prefactor  $b_1$  in the previous prediction: here we choose to calculate this value numerically for a surface structure at step  $n = 1$ , such as on Fig.1(a1). Using this calculated parameter as an input, a quantitative agreement is then found between the scaling prediction and the numerical results, as shown in Fig.3.

(ii) Case  $x = k/p = 1$ , i.e. fractal dimension  $d_f = 1$ : the



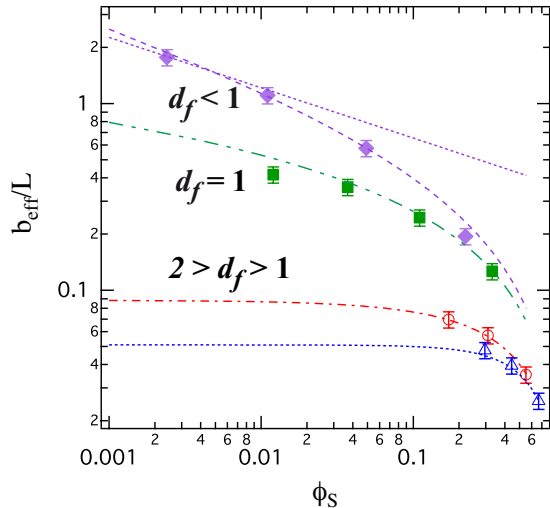


FIG. 3. Comparison between scaling law predictions and numerical results for 2D structures: normalized slip length  $b_{\text{eff}}/L$  as a function of the solid fraction  $\phi_s$  (in a log-log plot) for hierarchical fractal surfaces with different fractal dimensions  $d_f$ . Theoretical predictions of the scaling approach, Eq. (10), are shown as lines for the various fractal dimensions  $d_f$  under consideration (see text for details). Numerical results are from top to bottom: (i)  $d_f < 1$ :  $\{k,p\}=\{2,3\}$  ( $\blacklozenge$ ); (ii)  $d_f = 1$ :  $\{k,p\}=\{3,3\}$  ( $\blacksquare$ ); (iii)  $d_f > 1$ :  $\circ\{k,p\}=\{5,3\}$  and  $\triangle\{k,p\}=\{6,3\}$ . The top dotted line is the predicted asymptotic scaling in Eq.(20),  $b_{\text{eff}} \simeq \frac{3}{8}L \left(\frac{4}{\pi}\phi_s\right)^{-\alpha}$  with  $\alpha = (1 - d_f)/(2 - d_f)$ . Here  $\alpha \simeq 0.27$  for the fractal dimension  $d_f = 0.63$  corresponding to the hierarchical surface with  $\{k,p\}=\{2,3\}$ .

with  $\alpha = (1 - d_f)/(2 - d_f) \simeq 0.27$ . To be more precise, we show in Fig.3 (top dotted line) the analytical asymptotic prediction obtained in Eq.(20),  $b_{\text{eff}} \simeq \frac{3}{8}L \left(\frac{4}{\pi}\phi_s\right)^{-\alpha}$  with  $\alpha = (1 - d_f)/(2 - d_f)$ . This expression provides a result in good agreement with numerical results for small  $\phi_s$  [33]. Note however that in this case, the asymptotic (algebraic) scaling regime is still not fully reached for the smallest solid fraction considered. As can be seen from Eq.(10), the speed of convergence is actually fixed by the parameter  $x = p/k$ , which accounts for the sparsity of the structure: convergence to the scaling regime is accordingly faster for more sparse structure with  $x \gg 1$ , *i.e.* small  $d_f$ , while  $x = 3/2$  in the present case.

However, as we now show, a quantitative agreement can even be reached using the full expression in Eq.10 to evaluate the slip length. We use the numerical value for  $b_2$  at the  $n = 2$  iteration (with  $\phi_{s2} = 0.05$ ) as an input parameter to fix the prefactor for this law in order to compare to numerical results. With this reference value, the slip length takes the following expression  $b_{\text{eff}}(\phi_s) = b_2 \times (x^n - 1)/(x^2 - 1)$ , with  $n = \log(\phi_s)/\log(\phi_0)$ . As shown in Fig.3, this prediction is in quantitative agreement with the numerical results. Note that if one uses the  $n = 1$  iteration as a reference for the prefactor param-

eter, the agreement is slightly less good, as the scaling approach gives only a fair, semi-quantitative estimate to the slip length  $b_1$ .

Altogether the numerical results do confirm the theoretical predictions. A quantitative agreement can even be obtained by fixing the prefactor of the scaling behavior, using the numerical value of the slip length of the elementary structure (at the iteration  $n = 1$  or  $n = 2$ ).

Finally we consider in this paragraph the relationship between slippage and contact angle. The hierarchical fractal SH surface is characterized by its effective contact angle as defined in Eq.4 for a given iteration number  $n$ . We have plotted in Fig.4 the effective slip length as a function of  $\theta_{\text{eff}}$  for both hierarchical fractal SH surfaces and for SH surfaces made out of periodic posts (numerical results and scaling laws). Here we defined the effective contact angle as  $\theta_{\text{eff}} = \arccos(\phi_s - 1)$ , thus assuming for illustration purposes that the contact angle on the corresponding smooth surface is equal to  $\theta_0 = 90^\circ$ .

This plot illustrates immediately that the slip length is not a unique function of the contact angle  $\theta_{\text{eff}}$ : in contrast, it depends strongly on the geometry of the underlying structure for a given value of  $\theta_{\text{eff}}$ , as characterized here by various fractal dimensions  $d_f$ . The hydrodynamic properties of a SH surface and thus of a hierarchical fractal SH surface can not be simply determined from its effective contact angle. A strongly non-wettable surface with a contact angle of  $\theta_{\text{eff}} \simeq 180^\circ$  may well exhibit a low slip length and thus be inefficient in terms of drag reduction.

## B. Numerical results for slippage over hierarchical 1D structures

We finally turn to surfaces with 1D structures. We have plotted on Fig.5 the numerical results and the scaling laws for  $b_{\text{eff}}/L$  as a function of  $\phi_s$  (in log scale) for 1D hierarchical fractal SH surfaces characterized by different couples  $\{k,p\}$ . We have also plotted the analytical expression expected for a flow parallel to periodic grooves [14]. As for the 2D structures, the fractal surfaces yield values for the slip length which are far smaller than the one obtained on regular grooves. Furthermore as seen on this figure, we find a good agreement between the numerical results and the results of the scaling law approach. As for the 2D structure above, the prefactors for the scaling relationships are obtained by matching the slip length for the  $n = 2$  or  $n = 3$  iteration, as the scaling approach is expected to be valid for relatively small values of  $\phi_s$ .

## IV. CONCLUSION

In conclusion, we developed scaling laws for slippage on hierarchical fractal SH surfaces, providing explicit expressions for the slip length as a function of the solid

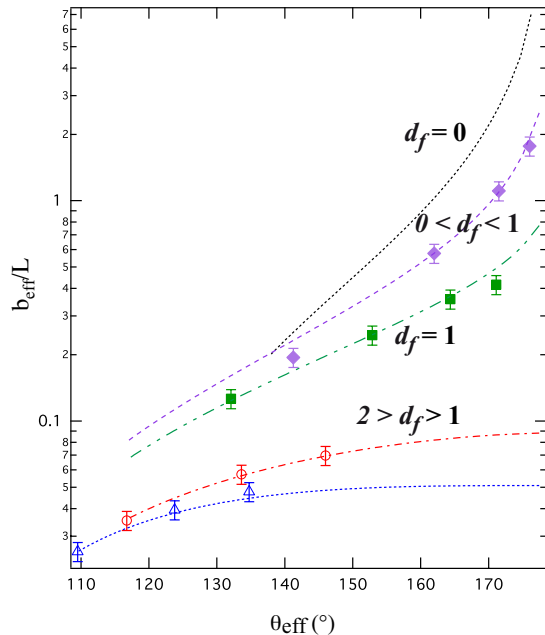


FIG. 4. Normalized effective slip length  $b_{\text{eff}}/L$  in logarithmic scales, as a function of the effective contact angle  $\theta_{\text{eff}}$  for different 2D SH surfaces. Symbols are the same as in Fig.3. The black dotted line (top) is the scaling law for SH surface made out of periodic posts as predicted from Ref. [29].

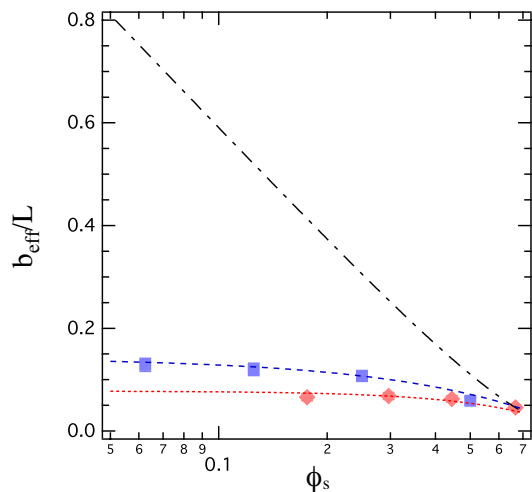


FIG. 5. Comparison between the numerical results and the scaling law approach for 1D structures: numerical results for the normalized slip length  $b_{\text{eff}}/L$  versus solid fraction  $\phi_s$ . Theoretical predictions of the scaling approach, Eq. (10), are shown as lines for the two systems under consideration (see text for details). Numerical results are from top to bottom:  $\{k,p\}=\{2,4\}$  (■);  $\{k,p\}=\{2,3\}$  (◆). The dash-dot line is the analytical solution for a flow parallel to periodic grooves as predicted in Ref. [14].

fraction  $\phi_s$  and fractal dimension  $d_f$  of the surface. For two dimensional structures, the slip length is found to scale as  $b_{\text{eff}} \sim \phi_s^{-\alpha}$  with  $\alpha = \frac{1-d_f}{2-d_f}$  and  $d_f$  the fractal dimension (here  $d_f = \log k / \log p$  for the hierarchical surfaces under consideration).

We checked the validity of this approach by numerical calculation of the full hydrodynamic equations. The numerical results show that the simple scaling description remains valid up to relatively high values of solid fractions, even though the scaling laws do not take properly into account the hydrodynamic interactions. A quantitative agreement can be obtained by fixing the prefactor of the scaling behavior, using the numerical value of the slip length of the elementary structure (at an iteration  $n = 1$  or  $n = 2$ ). For  $d_f \leq 1$  the scaling laws provide a good prediction for the slip length up to  $\phi_s = 0.1$  and for  $d_f > 1$  for which there is a fast saturation of the slip length, the agreement is good even for higher values of  $\phi_s$ . Globally the numerical results confirm that the scaling approach captures the physical mechanisms at play: although hydrodynamic interaction are neglected between posts, scaling results are shown to be predictive over a broad range of solid surface fraction.

Altogether, our study shows that for a given solid fraction  $\phi_s$ , fractal SH surfaces are less efficient than SH surfaces with regular pattern for drag reduction purposes. Furthermore for a given effective contact angle  $\theta_{\text{eff}}$ , the slip length on fractal SH surfaces decreases with increasing fractal dimension. This shows that slippage depends strongly on the geometry of the underlying structure for a given value of  $\theta_{\text{eff}}$  and the amount of slippage on a fractal SH surface can not just be determined from its effective contact angle. A strongly non-wettable surface with a contact angle close to  $180^\circ$  may well exhibit a low slip length and thus be totally inefficient in terms of drag reduction. This result is actually counter-intuitive: it shows that a surface with vanishingly small solid fraction leads to a finite friction force.

The use of fractal SH surfaces appears however as a good compromise between the positive effect of stabilization of the Cassie state and a moderate reduction of the slippage effect. Very large slip length and corresponding large drag reduction can indeed be observed on regular SH surfaces, but usually at the expense of a low stability of the Cassie state versus pressure. A recent study has demonstrated the recovery of the Cassie state after a transition towards the Wenzel state [34]. It would be thus interesting to consider surfaces with fractal structure in the context of stabilization issues [22].

Finally we mention that all results found in the present study for slip length can be immediately extended to heat transfer across fractal surfaces. In this case, the role of  $b_{\text{eff}}$  is played by the Kapitza resistance [18, 35], which quantifies the temperature slip at the surface between two different materials. A key point indeed is that the scaling arguments proposed here rely ultimately on the Laplacian nature of Stokes equation, so that all scaling results presented here do apply equally to any trans-



port property obeying a Laplacian equation, such as heat transport. Accordingly, one expects that the Kapitza resistance (and corresponding Kapitza length) at the interface with a hierarchical, fractal surface will obey similar scaling laws versus the solid fraction as the ones found here for the slip length: the Kapitza length is expected to scale as  $\phi_s^{-\alpha}$  with  $\alpha = (1 - d_f)/(2 - d_f)$  for surfaces with fractal dimension  $d_f < 1$  in the low  $\phi_s$  regime, while it is expected to saturate at a finite value for  $d_f > 1$ . This scaling results suggest therefore that for fractal dimensions  $d_f > 1$ , it may be possible to have a relatively low Kapitza surface resistance, thus maintaining a good heat transfer between the solid surface and the liquid, while keeping a strongly non-wetting superhydrophobic behavior. Such a compromise would be valuable for heat transfer problems in cooling pipes.

As an extension of this study, our results could also be applied in a different field to the question of trapping of diffusing particles by patchy surfaces [36], which is relevant to the questions of chemoreception and ligand binding to surface receptors [37, 38]. A counter-intuitive prediction emerging from our analysis is that in the regime of an effective fractal dimension  $1 < d_{\text{eff}} < 2$ , a hierarchical surface with *vanishingly small* surface fraction of receptors may yet result in a *finite* effective trapping rate.

## ACKNOWLEDGMENTS

We thank Elisabeth Charlaix, Jean-Louis Barrat and Christophe Ybert for many discussions on the subject. We acknowledge support from ANR, project *Mikado*.

- 
- [1] D., Quéré, “Non-sticking drops”, *Rep. Prog. Phys.* **68**, 2495 (2005).
- [2] L. Bocquet and E. Lauga “A smooth future?”, *Nature Mat.*, **10**, 334 (2011).
- [3] J. Bico, U. Thiele, and D. Quere, “Wetting of textured surfaces”, *Colloids Surf., A*, **206**, 41 (2002).
- [4] A. Lafuma and D. Quere, “Superhydrophobic states,” *Nature Mat.*, **2**, 457 (2003).
- [5] C. Cottin-Bizonne, J. L. Barrat, L. Bocquet, and E. Charlaix, “Low-friction flows of liquid at nanopatterned interfaces,” *Nat. Mater.*, **2**, 237 (2003).
- [6] D. Quere, A. Lafuma, and J. Bico, “Slippy and sticky microtextured solids,” *Nanotechnology*, **14**, 1109 (2003).
- [7] J. Ou, B. Perot, and J. P. Rothstein, “Laminar drag reduction in microchannels using ultrahydrophobic surfaces,” *Phys. Fluids*, **16**, 4635 (2004).
- [8] J. Ou and J. Rothstein, “Direct velocity measurements of the flow past drag-reducing ultrahydrophobic surfaces,” *Phys. Fluids*, **17**, 103606 (2005).
- [9] P. Joseph, C. Cottin, J.-M. Benoit, C. Ybert, C. Journet, P. Tabeling, L. Bocquet, “Slippage of water past superhydrophobic carbon nanotube carpets in microchannels”, *Phys. Rev. Lett.* **97** 156104 (2006).
- [10] C. Lee, C.H. Choi, C.J Kim, “Structured surfaces for a giant liquid slip”, *Phys. Rev. Lett.* **101** 064501 (2008).
- [11] S.S. Bahga, O.I. Vinogradova, M.Z. Bazant, “Anisotropic electro-osmotic flow over super-hydrophobic surfaces”, *J. Fluid Mech.* **644** 245 (2010)
- [12] C. Duez, C. Ybert, C. Clanet, L. Bocquet, “Wetting controls separation of inertial flows from solid surfaces”, *Phys. Rev. Lett.* **104** 084503 (2010).
- [13] A. Cassie and S. Baxter, “Wettability of porous surfaces”, *Trans. Faraday Society*, **40**, 546 (1944).
- [14] J. Philip, “Flows satisfying mixed no-slip and no-shear conditions,” *Z Angew Math Phys*, **23**, 353 (1972); *ibid.* “Integral properties of flows satisfying mixed no-slip and no-shear conditions”, **23**, 960 (1972).
- [15] E. Lauga and H. A. Stone, “Effective slip in pressure-driven stokes flow,” *J. Fluid Mech.*, **489**, 55 (2003).
- [16] E. Lauga, M. P. Brenner, and H. A. Stone, *Handbook of Experimental Fluid Dynamics*. Springer, New-York, 2005.
- [17] C. Navier, “Mémoire sur les lois du mouvement des fluides”, *Mémoires de l’Académie Royale des Sciences de l’Institut de France* **VI**.(1823).
- [18] L. Bocquet and J.-L. Barrat, “Flow boundary conditions from nano- to micro-scales”, *Soft Mat.* **3** 685 (2007)
- [19] S. Shibuichi, T. Onda, N. Satoh, and K. Tsujii, “Super water-repellent surfaces resulting from fractal structure”, *J Phys. Chem.*, **100**, 19512 (1996).
- [20] T. Onda, S. Shibuichi, N. Satoh, and K. Tsujii, “Superwater-repellent fractal surfaces”, *Langmuir*, **12** 2125 (1996).
- [21] H. E. Jeong, R. Kwak, J. K. Kim, and K. Y. Suh, “Generation and self-replication of monolithic, dual-scale polymer structures by two-step capillary-force lithography,” *Small*, **4**, 1913 (2008).
- [22] C. Lee and C.-J. C. Kim, “Maximizing the giant liquid slip on superhydrophobic microstructures by nanostructuring their sidewalls,” *Langmuir*, **25**, 12812 (2009)
- [23] Y. Kwon, N. Patankar, J. Choi, and J. Lee, “Design of surface hierarchy for extreme hydrophobicity,” *Langmuir*, **25**, 6129 (2009).
- [24] T. Liu, W. Sun, X. Sun, and X. Ai, “Thermodynamic Analysis of the Effect of the Hierarchical Architecture of a Superhydrophobic Surface on a Condensed Drop State” *Langmuir*, **26**:14835 (2010).
- [25] F. Feuillebois, M. Z. Bazant, and O. I. Vinogradova, “Effective Slip over Superhydrophobic Surfaces in Thin Channels”, *Phys. Rev. Lett.*, **102** 026001 (2009).
- [26] M. A. Samaha, H. V. Tafreshi, and M. Gad-El-Hak, “Modeling drag reduction and meniscus stability of superhydrophobic surfaces comprised of random roughness,” *Phys. Fluids*, **23**, 012001 (2011).
- [27] C. Lee and C.J. Kim “Influence of Surface Hierarchy of Superhydrophobic Surfaces on Liquid Slip” *Langmuir* **27**, 4243 (2011)
- [28] A. M. J. Davis and E. Lauga, “Hydrodynamic friction of fakir-like super-hydrophobic surfaces” *J. Fluid Mech.*, **661**, 402-411 (2010).
- [29] C. Ybert, C. Barentin, C. Cottin-Bizonne, P. Joseph, and L. Bocquet, “Achieving large slip with superhydrophobic surfaces: Scaling laws for generic geometries,” *Phys. Fluids*, **19**, 123601 (2007).

- [30] Note that in Ref.[29], the prefactor in front of the second term of the above equation, with  $b_s$ , was incorrect by a prefactor  $2\pi$  – cf. Eq(8) and Fig. 3 in this paper –, so that the correct prefactor in front of  $b_s$  is indeed close to unity..
- [31] J. Happel and H. Brenner, *Low Reynolds number hydrodynamics*, Kluwer, Dordrecht, The Netherlands (1983).
- [32] C. Cottin-Bizonne, C. Barentin, E. Charlaix, L. Bocquet, and J. Barrat, “Dynamics of simple liquids at heterogeneous surfaces: Molecular-dynamics simulations and hydrodynamic description,” *Eur Phys J E*, **15**, 427 (2004).
- [33] We note as a side remark that the numerical results are obtained for square-like posts, while the estimate of the prefactor is obtained for disk-like posts, in particular for the prefactor of Stokes law for disks,  $\chi = 16/3$ . However, these two estimates should differ only by a small amount: in Ref. [29], the numerical prefactor for  $b_{\text{eff}}/L$  vs  $\phi_s^{-1/2}$  for regular square-like posts structures was found to be 0.32, which is very close to the prediction in Eq.(19) for disks  $3\sqrt{\pi}/16 \simeq 0.33$ .
- [34] C. Lee and C.-J. Kim, “Underwater restoration and retention of gases on superhydrophobic surfaces for drag reduction”, *Phys Rev Lett*, **106**, 014502 (2011).
- [35] S. Merabia, S. Shenogin, L. Joly, P. Keblinski and J.-L. Barrat “Heat transfer from nanoparticles: A corresponding state analysis” *Proc. Nat. Acad. Sci.: USA* **106** 15113 (2009)
- [36] A. M. Berezhkovskii, Yu. A. Makhnovskii, M. I. Monine, V. Yu. Zitserman, and S. Y. Shvartsman, “Homogenization of boundary conditions on surfaces randomly covered by patches of different sizes and shapes” *J. Chem. Phys.* **121**, 11390 (2004).
- [37] H. C. Berg and E. M. Purcell, “Physics of chemoreception”, *Biophys. J.* **20**, 193 (1977).
- [38] D. Schoup and A. Szabo, “Role of diffusion in ligand binding to Macromolecules and cell-bound receptors” *Biophys. J.* **40**, 33 (1982).